Starvation mediates pancreatic cancer cell sensitivity to ferroptosis via ERK1/2, JNK and changes in the cell mesenchymal state

EGLE ZALYTE[1,2] and JONAS CICENAS[1,3]

[1]Proteomics Centre, Institute of Biochemistry, Vilnius University Life Sciences Centre;
[2]Institute of Biosciences, Vilnius University Life Sciences Centre, LT-10257 Vilnius, Lithuania;
[3]MAP Kinase Resource, Bioinformatics, CH-3027 Bern, Switzerland

Received January 22, 2022; Accepted April 5, 2022

DOI: 10.3892/ijmm.2022.5140

Abstract. Pancreatic cancer is a highly metastatic and therapy-resistant disease. In the present study, the prospects of a novel approach to kill pancreatic cancer cells were examined: Starvation combined with ferroptosis induction. Established pancreatic cancer cell lines (Miapaca2, Panc-1, Su.86.86 and T3M4), as well as a unique cell line, Capan-26, which was originally derived in the authors' laboratory, were used. Cells were deprived from growth factors, amino acids and pseudo-starved using treatment with mTOR inhibitors; erastin was used to induce ferroptosis. Cell viability and lipid peroxidation measurements using flow cytometry revealed that the starved pancreatic cancer cells reacted differently to ferroptosis induction: The Panc-1, Su.86.86 and T3M4 cells gained sensitivity, while the Miapaca2 cells acquired resistance. Fluorescence microscopy revealed that ERK1/2 translocated to the nucleus of the starved pancreatic cancer cells. Moreover, ERK1/2 pharmacological inhibition with SCH772984 prevented erastin-induced ferroptosis in the starved Panc-1, Su.86.86 and T3M4 cells. Confocal microscopy also indicated JNK activation. However, the inhibition of this kinase revealed its unexpected role in oxidative stress management: Treatment with the JNK inhibitor, SP600125, increased the viability of pseudo-starved cells following erastin treatment. In addition, the FBS-starved Miapaca2 and Capan-26 cells transitioned between epithelial and mesenchymal cell states. The results were further confirmed using wound healing assays, western blot analysis and microscopic analysis of epithelial-to-mesenchymal transition (EMT) markers. Mesenchymal properties were associated with a higher sensitivity to erastin, whereas epithelial-like cells were more resistant. Finally, it was demonstrated that compounds targeting EMT-related signaling pathways increased cell sensitivity to erastin. On the whole, these results confirm that in starved pancreatic cancer cells, ERK1/2 and JNK signaling, as well as switching between epithelial and mesenchymal states mediates sensitivity to erastin and reveal novel therapeutic prospects of the combination of starvation with ferroptosis induction.

Correspondence to: Dr Egle Zalyte, Institute of Biosciences, Vilnius University Life Sciences Centre, Sauletekio Avenue 7, LT-10257 Vilnius, Lithuania
E-mail: egle.zalyte@gf.vu.lt

Abbreviations: ROS, reactive oxygen species; FBS, fetal bovine serum; EMT, epithelial-to-mesenchymal transition

Key words: pancreatic cancer, ferroptosis, starvation, resistance, ERK1/2, JNK

Introduction

Pancreatic cancer is the seventh most common type of cancer worldwide. However, with only 6% successfully treated cases, it places fourth according to mortality rates (1). Delayed diagnosis and resistance to chemotherapy are the main causes of such a poor outcome. Early pancreatic cancer detection is limited by an asymptomatic disease and the lack of reliable diagnostic biomarkers. Locally advanced pancreatic tumors (30-40% of cases) can be surgically resected, and the procedure is often combined with chemo- or radiotherapy. However, it rarely leads to full tumor eradication (2). Metastatic pancreatic cancer has the worst prognosis, as it cannot be surgically removed and is highly resistant to traditional pancreatic cancer chemotherapeutic drugs, such as gemcitabine. Although several novel combination therapies (gemcitabine + nab-paclitaxel, gemcitabine + FOLFIRINOX) have been proposed in recent years (3,4), advanced pancreatic cancer still remains highly lethal. It is estimated that by the year 2025, pancreatic cancer may even reach the top three of the most lethal cancer types in Europe (5).

In 2012, a novel iron-dependent cell death form, ferroptosis, was identified (6). Cells that undergo ferroptosis die from excessive membrane lipid peroxidation. Fenton reactions and enzymes that use iron as a cofactor, such as lipoxygenases constantly generate lipid peroxides as a part of a normal cellular homeostasis. To prevent membrane damage, cells activate antioxidant enzyme glutathione peroxidase 4 (GPX4). The majority of ferroptosis inducers inhibit the activity or expression of GPX4, which leads to an oxidative membrane damage and eventual cell death. In recent years, ferroptosis has been researched in the context of cardiovascular and

neurodegenerative diseases, as well as tissue injury and cancer (7). Of note, as cancer cells have more soluble iron in their cytosol than their normal counterparts, they require a milder oxidative stimulus to induce ferroptosis. Thus, ferroptosis can be specifically targeted to malignant cells, particularly in iron-addicted cancers (8). Apart from an upregulated iron metabolism, other factors can also predetermine sensitivity to ferroptosis. For example, in pancreatic cancer, susceptibility to ferroptosis is associated with constitutive *KRAS* activation (9). Indeed, the first known ferroptosis inducers, erastin and RSL3, were originally discovered as compounds selectively lethal to *RAS*-mutated cancer cells. Moreover, it has been shown that therapy-resistant and metastatic cancer cells are particularly sensitive to ferroptosis induction (10,11). The vulnerability of metastatic cancer to ferroptosis may be attributed to an increased polyunsaturated fatty acid content in cell membranes, which renders them an easy target of oxidation and elicits dependency on GPX4 (12,13). In addition, resistance to ferroptosis inducers is coupled with metabolic reprograming and glutamine/glucose dependency (14). Pancreatic cancer also falls into a broad category of glutamine-dependent cancer (15).

The question why tumors metastasize has not yet been fully answered. Metastasis does not appear to be predetermined genetically, and although certain genetic mutations promote metastasis, environmental factors play a major role (16). From an evolutionary perspective, it can be hypothesized that cells increase their motility in order to migrate towards a more favorable growth environment (for example, more nutrient-rich). Such behavior is common for bacteria and certain primitive eukaryotes (17,18). However, the atavistic point of view does not necessarily fit complex systems, as tumors can develop adaptive mechanisms. When starved, cancer cells use alternative energy sources, micropinocytosis, metabolic symbiosis, autophagy, increase nutrient supply via angiogenesis and vessel co-option (19-25). Nevertheless, several studies suggest that a dysregulated microenvironment, such as extensive cell death, pH changes due to the Warburg effect, signals from stromal and immune cells can induce and enhance metastasis (26-30). From this point of view, nutrient and growth factor deprivation are also metastatic triggers. Moreover, metastasis itself can be viewed as a form of adaptation. In recent years, efforts have been put forth into developing therapies that collectively exploit metabolic vulnerabilities of metastatic cancer. However, care should be taken to avoid an adaptive response, which would elicit an opposing, cancer-promoting result.

The present study unveils novel (to the best of our knowledge) molecular mechanisms through which starvation mediates resistance to ferroptosis in pancreatic cancer cells and proposes ferroptosis modulation strategies with which to improve pancreatic cancer treatment.

Materials and methods

Cell culture and treatments. In the present study, five human ductal adenocarcinoma cell lines were used: Miapaca2, Panc-1, Su.86.86, T3M4 and Capan-26. The Miapaca2 cell line was a kind gift from Dr Vitalijus Karabanovas (Biomedical Physics Laboratory, National Cancer Institute, Vilnius, Lithuania). The Panc-1, Su.86.86 and T3M4 cells were gifts from Dr Arvydas Kanopka (Department of Immunology and Cell Biology, Institute of Biotechnology, Life Sciences Center, Vilnius, Lithuania). The Capan-26 cell line was previously established in the authors' laboratory using an explant method and characterized by assessing the doubling time, tumor and stem cell marker expression, colony forming efficiency, mutations of the *KRAS* and *TP53* genes, karyotype and sensitivity to drug treatment (31). To summarize the main findings, Capan-26 expresses the pancreatic cancer markers, CEA cell adhesion molecule 6 and carbohydrate antigen 19-9, the epithelial marker, E-cadherin, as well as the stem cell markers, CD44, octamer-binding transcription factor 4 and zinc finger E-box binding homeobox 1. The cells successfully form colonies in soft agar. Additionally, Capan-26 bears a deletion of *KRAS* exon 3 and a Val172Phe point mutation V172F in *TP53* exon 5. It is a mixed aneuploid/polyploid population. All cell lines tested negative for mycoplasma.

The Miapaca2, Panc-1, Su.86.86 and T3M4 cells were cultured in DMEM (Gibco; Thermo Fisher Scientific, Inc.), supplemented with 10% FBS (Gibco; Thermo Fisher Scientific, Inc.) and 1% penicillin/streptomycin (Gibco; Thermo Fisher Scientific, Inc.). The Capan-26 cells were cultured in Iscove's modified Dulbecco's medium (Gibco Thermo Fisher Scientific, Inc.) with 10% FBS and 1% penicillin/streptomycin. Cells were grown at 37˚C in a humidified atmosphere with 5% CO_2. For all experiments, cells were seeded at the following densities: Miapaca2, $8x10^4$ cells/ml; Panc-1 and Su.86.86, $7x10^4$ cells/ml; T3M4, $9x10^4$ cells/ml. The Capan-26 cells were split 3-4 times.

EGFR inhibitor, afatinib (Afa, 1 μM), FGFR inhibitor, BGJ398 (BG, 1 μM), ferroptosis inducer, erastin (Era, 0.4-20 μM), the ferroptosis inhibitor, ferrostatin-1 (Ferr-1, 1 μM), the dual mTORC1/mTORC2 inhibitor, INK128 (INK, 0.125 nM), the ERK1/2 inhibitor, SCH772984 (SCH, 1 μM), the FAK inhibitor, PF573228 (PF, 2 μM), the Src inhibitor, saracatinib (Sar, 2 μM), the YAP antagonist, super-TDU (TDU, 0.2 μM), the mammalian sterile 20-like kinase (MST)1/2 inhibitor, XMU-MP-1 (XMU, 5 μM), the glycogen synthase kinase (GSK)-3 inhibitor, tideglusib (TDG, 5 μM), and the IKK inhibitor, TPCA (5 μM), were purchased from Selleck Chemicals. The tankyrase inhibitor, XAV939 (XAV, 5 μM), the JNK inhibitor, SP600125 (SP6, 5 μM), and the Unc-51 like autophagy activating kinase 1 (ULK-1) inhibitor, SBI-0206965 (SBI, 1 μM), were purchased from MilliporeSigma. The mTORC1 inhibitor, rapamycin (Rap, 0.25 nM), was obtained from Santa Cruz Biotechnology, Inc. The caspase inhibitor, Z-VAD-FMK (ZVAD, 1 μM), was purchased from R&D Systems, Inc. The RIPK1 inhibitor, necrostatin-1 (Nec-1, 1 μM), was purchased from Alfa Aesar. All compounds were dissolved in dimethyl sulfoxide (DMSO), stored at -20˚C and diluted in growth medium to their final concentrations immediately prior to use. An appropriate volume of DMSO was used as a vehicle in control cells.

The EGF and bFGF (100 ng/ml) recombinant proteins were purchased from Invitrogen and stored according to manufacturer's instructions.

Cell viability assessment. Cell viability was evaluated using propidium iodide (PI) staining. The day before treatment, the cells were seeded into 48-well plates (SigmaAldrich; Merck KGaA). Combined treatments were administered sequentially:

First, the cells were treated with inhibitors for 1 h, and erastin was then added to the culture medium. Overall, the cells were exposed to the treatments for 48 h. The substratum-bound and detached cells were then collected, centrifuged at 600 x g for 3 min at room temperature, suspended in PBS and stained with 0.5 μg/ml PI for 5-10 min. The proportion of cells with a permeabilized membrane was determined using the Guava easyCyte 8HT flow cytometer (MilliporeSigma). If the proportion of apoptotic (caspase-3/7-positive) cells was to be evaluated simultaneously, the cells were also stained with Caspase-3/7 Green detection reagent (Invitrogen; Thermo Fisher Scientific, Inc.; 0.5 μM; 37˚C for 30 min). The data were analyzed using Flowing Software 2.5.1 (University of Turku, Turku, Finland).

Detection of membrane lipid oxidation using C11-BODIPY 581/591 staining. To detect cells with oxidized membrane lipids, the cells were starved by culturing without FBS, without amino acids L-glutamine, L-lysine and L-arginine or treated with Rap and simultaneously exposed to erastin and/or Ferr-1, then stained with 0.5 μM C11 BODIPY 581/591 fluorescent probe (Invitrogen; Thermo Fisher Scientific, Inc.) for 30 min at room temperature. The cells were then collected, centrifuged at 600 x g for 3 min at room temperature, resuspended in PBS and analyzed on the Guava easyCyte 8HT flow cytometer (MilliporeSigma). Data analysis was performed using Flowing Software 2.5.1 (University of Turku).

Oxidized membrane lipids in Capan-26 cells were visualized using confocal microscopy. Briefly, the cells were seeded on glass coverslips, stained with 10 μM C11 BODIPY 581/591 for 30 min at 37˚C, washed with PBS, mounted in Prolong Gold Antifade reagent (Molecular Probes; Invitrogen; Thermo Fisher Scientific, Inc.) and observed immediately using a confocal laser scanning microscope (Eclipse TE2000-S; Nikon Corporation).

Fluorescence/confocal microscopy. For immunofluorescence experiments, the cells were seeded on glass coverslips in 24-well plates (MilliporeSigma). After 24 h, the cells were treated with the corresponding compounds, washed twice with PBS and fixed with 4% paraformaldehyde (15 min at room temperature). The cells were then washed three times with 1% BSA (MilliporeSigma) in PBS and permeabilized with 0.2% of Triton X-100 (MilliporeSigma) in PBS (15 min at room temperature). After washing, the non-specific binding sites were blocked by incubating with 1% BSA in PBS at room temperature for 30 min. The coverslips were then stained with the following primary antibodies for 1 h at 37˚C: Rabbit anti-ERK1/2 (1:100; produced in the authors' laboratory by rabbit immunization with a recombinant protein), rabbit anti-phospho-JNK (1:400; cat. no. V7931; Promega Corporation), rat anti-E-cadherin (1:400; cat. no. 13-1900; Thermo Fisher Scientific, Inc.), followed by washing with 1% BSA in PBS five times and 30 min of incubation at 37˚C with Alexa Fluor™ 594-conjugated anti-rabbit (H+L) or Alexa Fluor™ 594-conjugated anti-rat (H+L) secondary antibodies (both 1:250; cat. nos. A32740 and A-11007, respectively; Thermo Fisher Scientific, Inc.). Cell nuclei were stained with 300 nM 4',6-diamidino-2-phenylindole dihydrochloride (DAPI) dye (Thermo Fisher Scientific, Inc.) for 10 min at room temperature. After washing, the coverslips were mounted in Prolong Gold antifade (Molecular Probes; Invitrogen) and observed using a confocal laser scanning microscope (Eclipse TE2000-S; Nikon Corporation). Fluorescence intensity in the cell nuclei was quantified using ImageJ 1.52v software (National Institutes of Health).

Western blot analysis. The cells were washed with PBS and lysed on ice in EB++ lysis buffer (extraction buffer; 10 mM Tris-HCl, pH 7.4, 1 mM Tris base, 50 mM NaCl, 50 mM NaF, 1% Triton X-100, 5 mM EDTA, 2 mM Na_3VO_4 and 1 mM PMSF; pH 7,2-7,4). The cell lysates were centrifuged 20,000 x g for 15 min at 4˚C. The protein concentration was quantified as previously described (32). Protein samples were subjected to 12% SDS-PAGE, transferred to polyvinylidene difluoride membranes (Bio-Rad Laboratories, Inc.) by wet transfer and blocked in blocking buffer containing 1% milk powder (45 min, room temperature). The membranes were then incubated with primary mouse anti-vimentin (1:2,000; cat. no. 550513; BD Pharmingen™) and mouse anti-YAP1 (1:500; cat. no. sc-101199; Santa Cruz Biotechnology, Inc.) antibodies for 2 h at room temperature. In addition, the blots were probed with mouse anti-GAPDH antibody (1:1,000; cat. no. AM4300; Thermo Fisher Scientific, Inc.) for the detection of GAPDH as a loading control. After washing four times for 5 min at room temperature with 0.1% Tween-20 (Carl Roth Gmbh & Co. Kg) in PBS (PBS-T), membrane-bound primary antibodies were probed with IRDye® 800CW Infrared dye conjugated secondary goat anti-mouse antibody (1:10,000; cat. no. 926-32210; LI-COR Biosciences) for 30 min at room temperature. After washing again for four times with PBS-T and once with PBS, the membranes were scanned on an Odyssey® Infrared Imaging System (LI-COR Biosciences). Densitometric analysis was performed using ImageJ 1.52v software (National Institutes of Health).

Wound healing assay. The cells were seeded in 24-well plates (MilliporeSigma) and cultured until they reached confluency. In one group, a scratch was made using a sterile 10 μl pipette tip, and the cells were washed with PBS and supplemented with fresh medium without FBS. In the other group, cells were FBS-starved for an additional 4 days, and a scratch was then made. In both cases, images of the same three fields were captured using an Eclipse TE2000-S microscope (Nikon Corporation; magnification, x10) at 0 and 48 h after scratching. The width of the healed wound was calculated using the ImageJ 1.52v plugin MRI Wound Healing Tool (National Institutes of Health).

Glutathione (GSH) assay. GSH levels were determined in the cells using Ellman's reagent (5,5-dithio-bis-(2-nitrobenzoic acid) (DTNB; MilliporeSigma). The cells were collected, centrifuged at 400 x g for 4 min at room temperature and resuspended in PBS. Subsequently, one-tenth of the cell suspension was used for cell counting using a Guava easyCyte 8HT flow cytometer (MilliporeSigma). The remaining cells were centrifuged again at the same conditions as in the previous step and resuspended in 20 μl working buffer (100 mM Tris-HCl; 1 mM EDTA). To precipitate proteins, 20 μl 5% trichloroacetic acid were added, and the samples

were incubated on ice at 4˚C for 15 min. Acid was neutralized with 5 μl 2 M Tris base. The samples were then centrifuged at 12,000 x g for 5 min at room temperature, and 1.5 mM of DTNB was added to the supernatant. The absorbance was measured at 412 nm with Varioskan Flash Multimode Reader (Thermo Fisher Scientific, Inc.). The GSH level was calculated according to the calibration curve prepared with pure GSH (Carl Roth Gmbh & Co. Kg) and normalized to the cell number in each sample.

Statistical analysis. Microsoft Office Excel (v16.0) software was used for statistical analysis. The data are presented as the mean ± standard deviation from at least three independent assays, each one at least in duplicate. The unpaired Student's t-test was used to compare two groups. Multiple comparisons were performed using Tukey post-hoc test, following one-way ANOVA. $P<0.05$ was considered to indicate a statistically significant difference.

Results

Starved pancreatic cancer cells react differently to ferroptosis induction. In eukaryotic cells, the main sensor of environmental conditions is mTOR (33). As mTOR signaling mediates both adaptation to nutrient/growth factor deprivation and oxidative stress, the interplay between pharmacological mTOR inhibition and sensitivity to erastin-induced ferroptosis was first analyzed. Cell viability following erastin treatment was examined in a panel of pancreatic cancer cell lines cultured in standard medium in the absence of FBS, L-glutamine, L-lysine and L-arginine (33) and pseudo-starved by exposing them to the mTOR inhibitors, Rap and INK (Fig. 1A-D). Starvation elicited contrasting responses in different cell lines. In the mesenchymal-like Miapaca2 cells, FBS, amino acid starvation and rapamycin treatment prevented cell death. By contrast, in the epithelial-like Panc-1 and Su.86.86 cells, ferroptosis was strongly induced. Pseudo-starvation induced by rapamycin exerted the most prominent effect, whereas amino acid starvation slightly decreased the viability of the control cells, although this was not due to ferroptosis. The dual mTORC1/mTORC2 inhibitor, INK, on the other hand, did not affect sensitivity to ferroptosis, apart from the Panc-1 cells. Lipid peroxidation detection by C11 BODIPY staining was also performed. Unless otherwise stated, for the Miapaca2 and Panc-1 cell lines, the proportion of the oxidized population was quantified (Fig. S1). For the Su.86.86 and T3M4 cells, the medium fluorescence intensity was analyzed. C11 BODIPY staining supported the cell viability results (Fig. 1E-H). In the T3M4 cells, FBS withdrawal increased the proportion of oxidized membrane lipids, as well as cell death following erastin treatment. However, Ferr-1 did not prevent erastin-induced T3M4 cell death and neither did the inhibitors of apoptosis, necroptosis or autophagy (Fig. S2A). Erastin also failed to elevate the proportion of apoptotic (caspase-3/7$^+$) cells (Fig. S2B). Such results indicate a partial change in the cell death type following erastin treatment and overall stronger ROS-adaptive mechanisms in T3M4 cells. Taken together, these data suggest the differential regulation of the erastin-induced ferroptosis of starved pancreatic cancer cells.

Starvation regulates ferroptosis via ERK1/2. The inability of the selective mTORC1/mTORC2 inhibitor, INK, to induce changes in pancreatic cancer cell viability in contrast to the mTORC1 inhibitor, rapamycin, strongly suggests the involvement of mTORC2-mediated feedback loops. One of the possible mTORC2 targets is ERK1/2. Although Soares *et al* (34) demonstrated that prolonged incubation with rapamycin did not activate ERK1/2 in pancreatic cancer cells, ERK1/2 translocated to the nucleus in cells starved for a short period of time and/or treated with erastin (Figs. 2 and S3). Rapamycin and erastin synergistically promoted ERK1/2 translocation to the nucleus in the Miapaca2, Panc-1, Su.86.86 and T3M4 cells. ERK1/2 also translocated to the nucleus of FBS and amino acid-deprived control Panc-1 cells (not treated with erastin); however, as erastin itself enhanced ERK1/2 translocation, there was no significant difference in the fluorescence intensity in the nucleus of the erastin-treated control and starved cells. In the control Miapaca2 cells, FBS and amino acid starvation also resulted in ERK1/2 translocation; however, erastin did not enhance this effect. To further elucidate the role of ERK1/2 in ferroptosis, this kinase was inhibited with its inhibitor, SCH, and it was then examined whether sensitivity to erastin was affected in starved pancreatic cancer cells (Fig. 3A-D). The results suggested that ERK1/2 inhibition increased the viability of rapamycin-treated and FBS-deprived Panc-1 and Su.86.86 cells. Moreover, SCH failed to rescue the starved cells from lipid oxidation following exposure to a higher erastin concentration (Figs. 3E-H and S4). In the Miapaca2 cells, SCH treatment did not reverse starvation-induced erastin resistance either. Collectively, these data indicate that ERK1/2 primes starved Panc-1, Su.86.86 and T3M4 cells for erastin-induced ferroptosis.

Starvation regulates ferroptosis via JNK. The c-Jun transcription factor is another regulator of anti-oxidative stress responses and is activated by JNK. In the present study, phospho-JNK immunofluorescence revealed that erastin treatment activated JNK only in Miapaca2 cells (Fig. 4A). However, starvation alone induced JNK phosphorylation in all four cell lines. JNK activation was prominent following FBS and amino acid starvation and with rapamycin treatment in the Miapaca2 and Su.86.86 cells, following FBS withdrawal and rapamycin treatment in Panc-1 cells and following FBS and amino acid starvation in T3M4 cells. Of note, treatment with the JNK inhibitor, SP6, prevented the ferroptosis of cells exposed to rapamycin (Fig. 4B-E). JNK inhibition reduced cell viability under standard conditions only in Panc-1 cells, although its activation was not observed in immunofluorescence experiments, which suggests delayed JNK activation in these cells. These data highlight a novel role for JNK in oxidative stress responses: In starved pancreatic cancer cells, JNK activation elevates erastin-induced ferroptosis.

Pancreatic cancer cells transition between different mesenchymal states during FBS starvation. The results of the present study indicated that starvation elicited opposing effects in Miapaca2 cells and in the other tested cell lines, Panc-1, Su.86.86 and T3M4. When starved, the Miapaca2 cells acquired resistance to erastin, rather than sensitivity. Notably, starvation provoked changes in the Miapaca2 cell

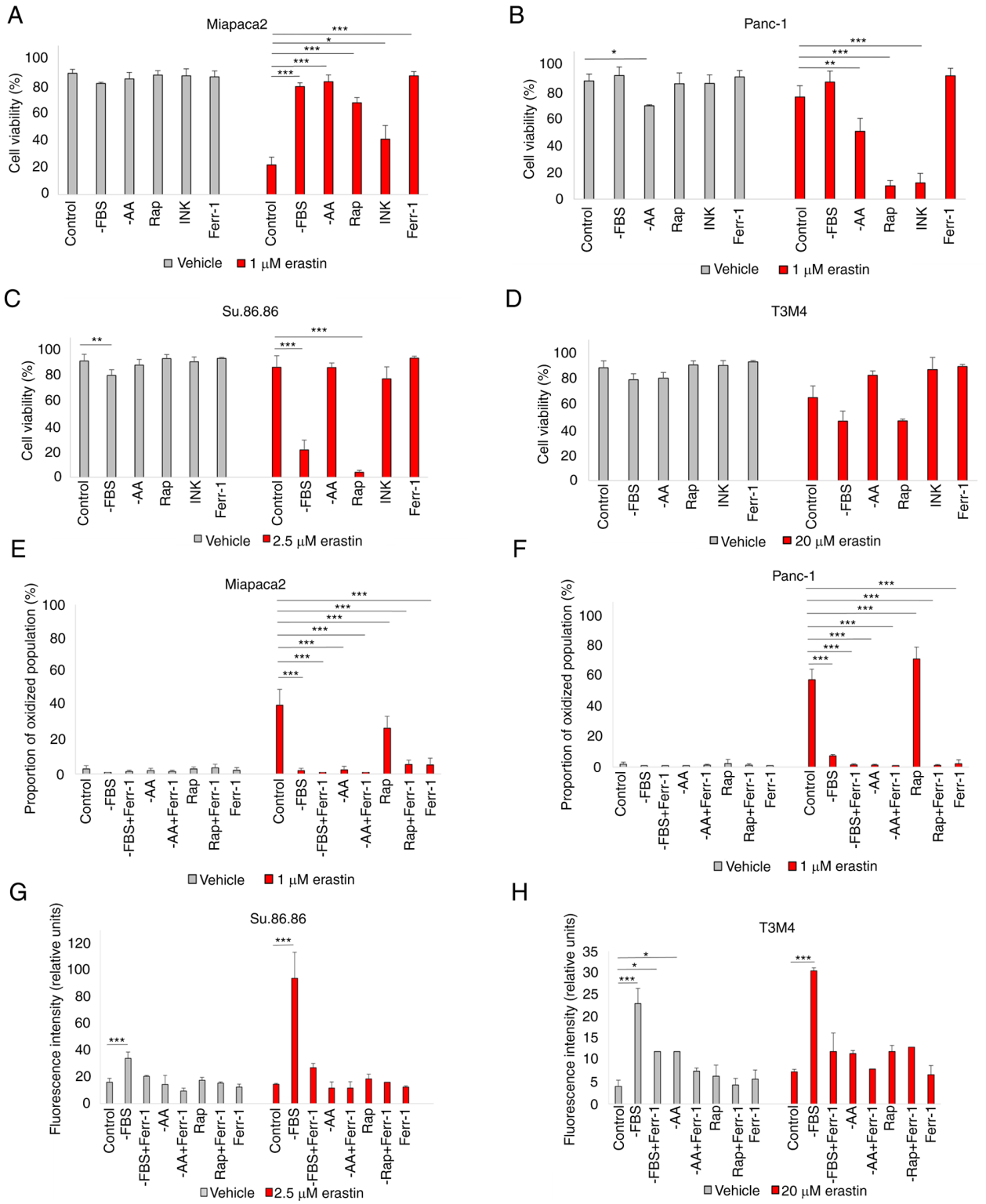

Figure 1. Starved pancreatic cancer cells react differently to ferroptosis induction. (A-D) Viability assessment of (A) Miapaca2, (B) Panc-1, (C) Su.86.86 and (D) T3M4 cells cultured without FBS, without the amino acids L-glutamine, L-lysine and L-arginine or pseudo-starved using treatment with the mTOR inhibitors rapamycin (0.25 nM) and INK (0.125 nM). (E-H) Measurement of lipid peroxidation of (E) Miapaca2, (F) Panc-1, (G) Su.86.86 and (H) T3M4 cells cultured without FBS, L-glutamine, L-lysine and L-arginine and pseudo-starved using treatment with rapamycin (0.25 nM). Ferroptosis was induced by erastin and inhibited by Ferr-1. The data are presented as the mean ± SD; n=3. Cells cultured under standard conditions were used as the control. *P<0.05, **P<0.01 and ***P<0.001, vs. control. -AA, cells, cultured without L-glutamine, L-lysine and L-arginine; Rap, rapamycin; INK, INK128; Ferr-1, ferrostatin-1.

growth pattern and morphology: After growing without FBS for 2 days, the originally mesenchymal-like Miapaca2 cells formed islands, characteristic of epithelial cells; however, after a 5-day starvation period, they become spindle-shaped (Fig. 5A). Therefore, it was hypothesized that these morphological changes may indicate transitioning between epithelial and mesenchymal cell states. Indeed, wound healing assays revealed that during the first 2 days of starvation, the cells were

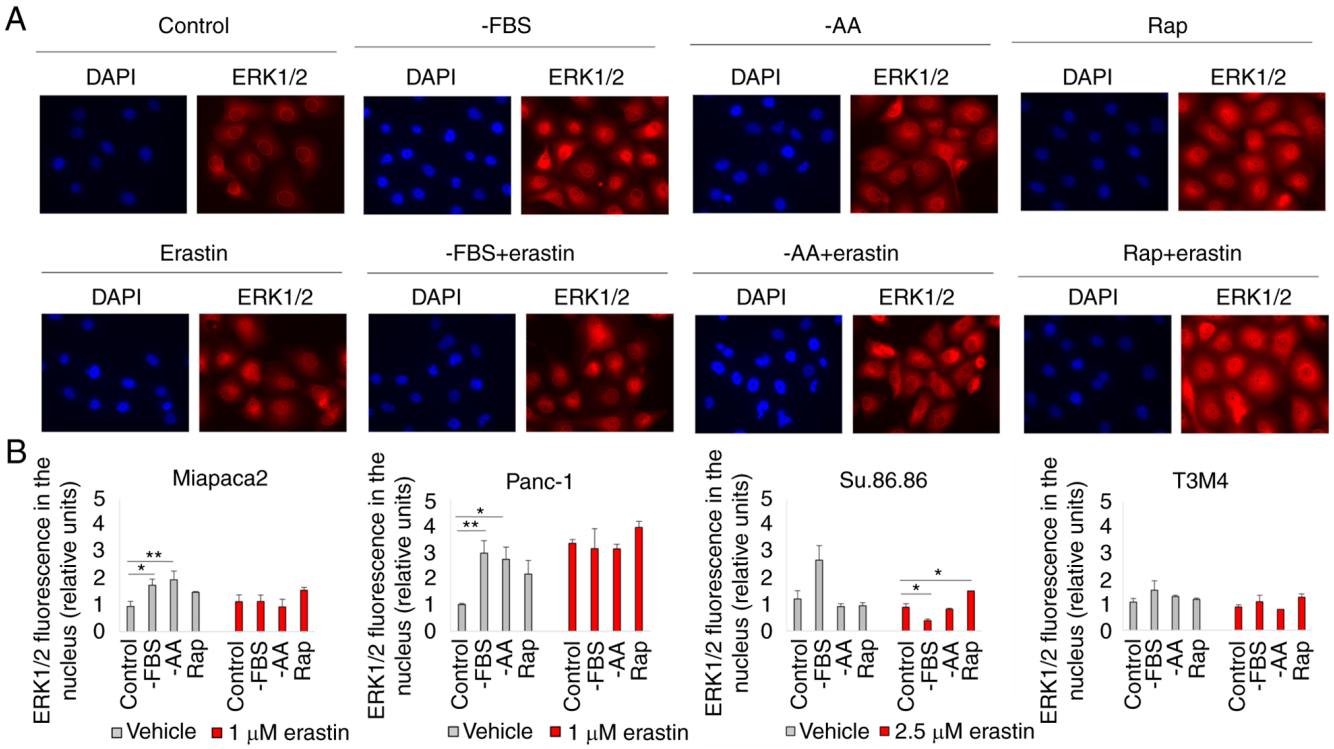

Figure 2. ERK1/2 is translocated to the nucleus in starved pancreatic cancer cells. (A) Representative fluorescence microscopy images of (pseudo)starved (rapamycin-treated) Panc-1 cells, with or without erastin treatment. Magnification, x20. (B) Quantification of the fluorescence intensity in cell nucleus of (pseudo)starved (Rap-treated) Miapaca2, Panc-1, Su.86.86 and T3M4 cells. The data are presented as the mean ± SD; n=3. Cells cultured under standard conditions were used as the control. *P<0.05 and **P<0.01 vs. control. -AA, cells, cultured without L-glutamine, L-lysine and L-arginine; Rap, rapamycin.

about as twice less motile as during days 4-6 of starvation (Fig. 5B and C). Western blot analysis was used to examine the expression of the mesenchymal markers, vimentin and YAP1, which confirmed that the expression of vimentin and YAP1 was the lowest on day 2 of FBS starvation, and the highest on day 5 (Figs. 5D and E, and S5A and B). No similar changes in plasticity were observed in the Panc-1, Su.86.86 and T3M4 cell lines, which are originally more epithelial-like in nature (Fig. S6). However, the Capan-26 cell line, which was established and characterized as an epithelial pancreatic cancer cell line in the authors' laboratory, exhibited similarities to the Miapaca2 cells. Indeed, after 3 days of FBS starvation, the cells at the edge of the islands acquired a mesenchymal shape (Fig. 5F) and lost membrane E-cadherin expression (Fig. 5G). However, vimentin expression did not increase during starvation, possibly because only a small population of cells was affected (Fig. S5C). With respect to ferroptosis, the Miapaca2 cells on day 2 of FBS starvation (most epithelial-like) were about twice less sensitive to erastin than on day 5 (most mesenchymal-like) (Fig. 6A). The Capan-26 cells were overall very resistant to erastin, although erastin treatment following a 3-day starvation period induced lipid oxidation (Fig. 6B and C). However, Ferr-1 failed to reduce membrane oxidation. C11 BODIPY microscopy clearly identified oxidized lipids in the membranes of mesenchymal-shaped cells at the edges of starved cell islands, compared with a non-starved control (Fig. 6D). Together, these data indicate that in Miapaca-2 and Capan-26 cells, starvation promotes transitioning between mesenchymal and epithelial states, with the mesenchymal state being more sensitive to ferroptosis induction than the epithelial state.

Modulation of epithelial-to-mesenchymal transition (EMT) can be used to increase pancreatic cancer cell sensitivity to ferroptosis. The aforementioned results encouraged the exploration of the possibilities of ferroptosis modulation in EMT-prone mesenchymal-like pancreatic cancer cells. A combinatorial cell viability analysis of erastin and EMT-targeting compounds in FBS-starved and non-starved cells was performed. Firstly, the EMT-inducing growth factors, EGF and bFGF, sensitized the Miapaca2 cells to erastin under standard conditions, and had no significant effect on cells cultured in the absence of FBS for 2 days (most epithelial-like state) (Fig. 7A). The sensitivity-inducing effect was completely abolished by treating the cells with the EGFR and FGFR inhibitors, afatinib and BGJ398, respectively. Secondly, two anti-EMT agents, the Src inhibitor, Sar, and the functionally similar FAK inhibitor, PF, were tested for their effects on ferroptosis. Sar completely rescued the Miapaca2 cells from erastin-induced cell death, alone or in combination with PF, although PF did not affect cell viability (Fig. 7B). Finally, other compounds, which are not conventional EMT-targeted drugs, but modulate EMT-related signaling pathways, were also tested in the Miapaca2, Panc-1, Su.86.86 and T3M4 cells: NF-κB (IKK inhibitor, TPCA), Wnt (tankyrase inhibitor, XAV, and GSK-3 inhibitor, TDG) and Hippo (MST 1/2 inhibitor, XMU) (Fig. 7C). Wnt and Hippo signaling inhibition increased cell sensitivity to erastin, in most cases at a high erastin concentration. The combination

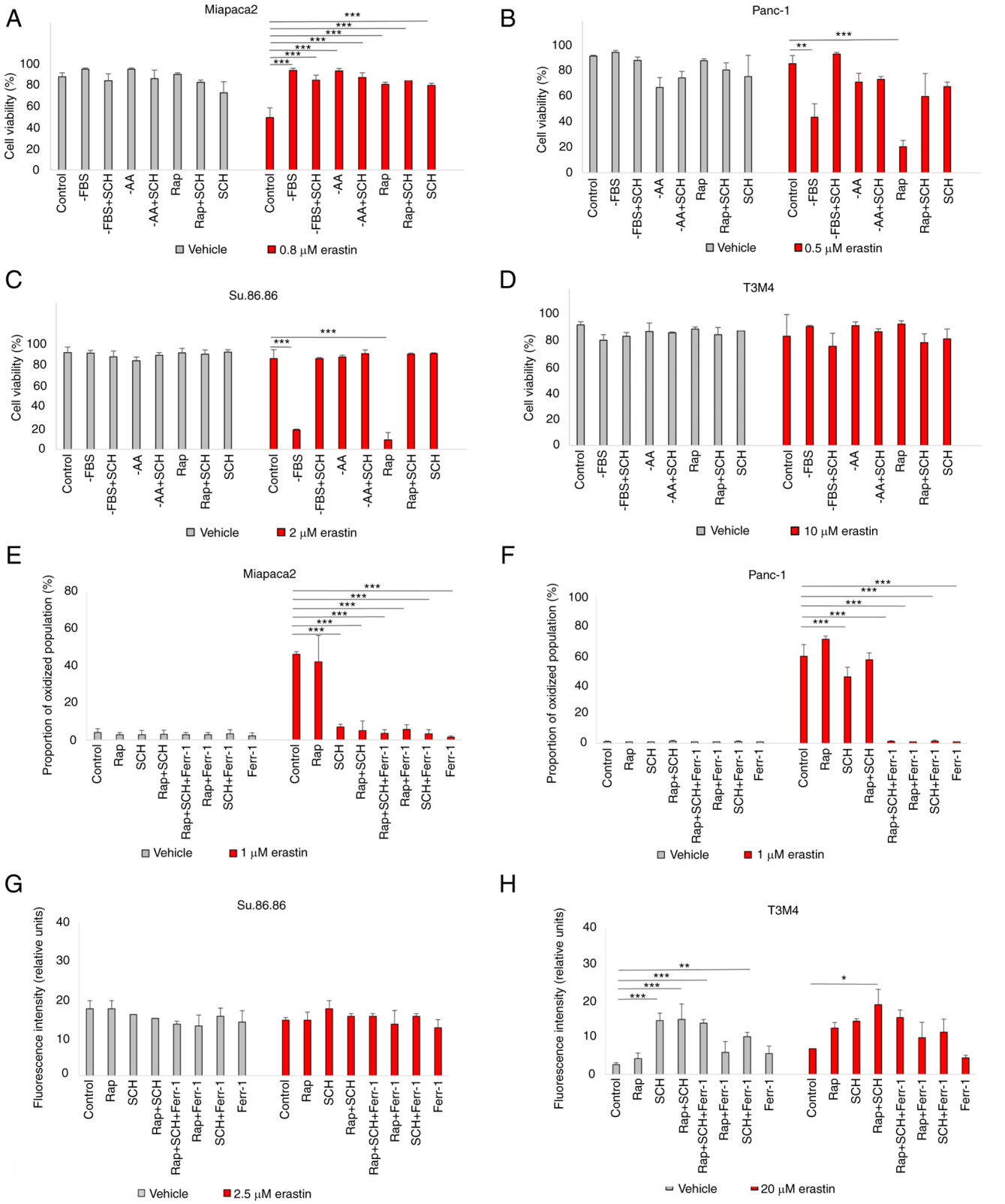

Figure 3. Starvation regulates ferroptosis via ERK1/2. (A-D) Cell viability assessment of (A) Miapaca2, (B) Panc-1, (C) Su.86.86 and (D) T3M4 cells cultured without FBS, without amino acids L-glutamine, L-lysine and L-arginine, pseudo-starved by treating with Rap and treated with the ERK1/2 inhibitor, SCH (1 μM). (E-H) Measurement of lipid peroxidation of pseudo-starved (E) Miapaca2, (F) Panc-1, (G) Su.86.86 and (H) T3M4 cells. Ferroptosis was induced by erastin and inhibited by Ferr-1. The data are presented as the mean ± SD; n=3. Cells cultured under standard conditions were used as the control. *P<0.05, **P<0.01 and ***P<0.001, vs. control. -AA, cells, cultured without L-glutamine, L-lysine and L-arginine; Rap, rapamycin; SCH, SCH772984; Ferr-1, ferrostatin-1.

of erastin and TDG exerted the most prominent cytotoxic effect under standard conditions in all cell lines tested, even in T3M4 cells, which are overall resistant to erastin. These data indicate that pancreatic cancer cell sensitivity to ferroptosis can be modulated and promoted using EMT-targeting compounds.

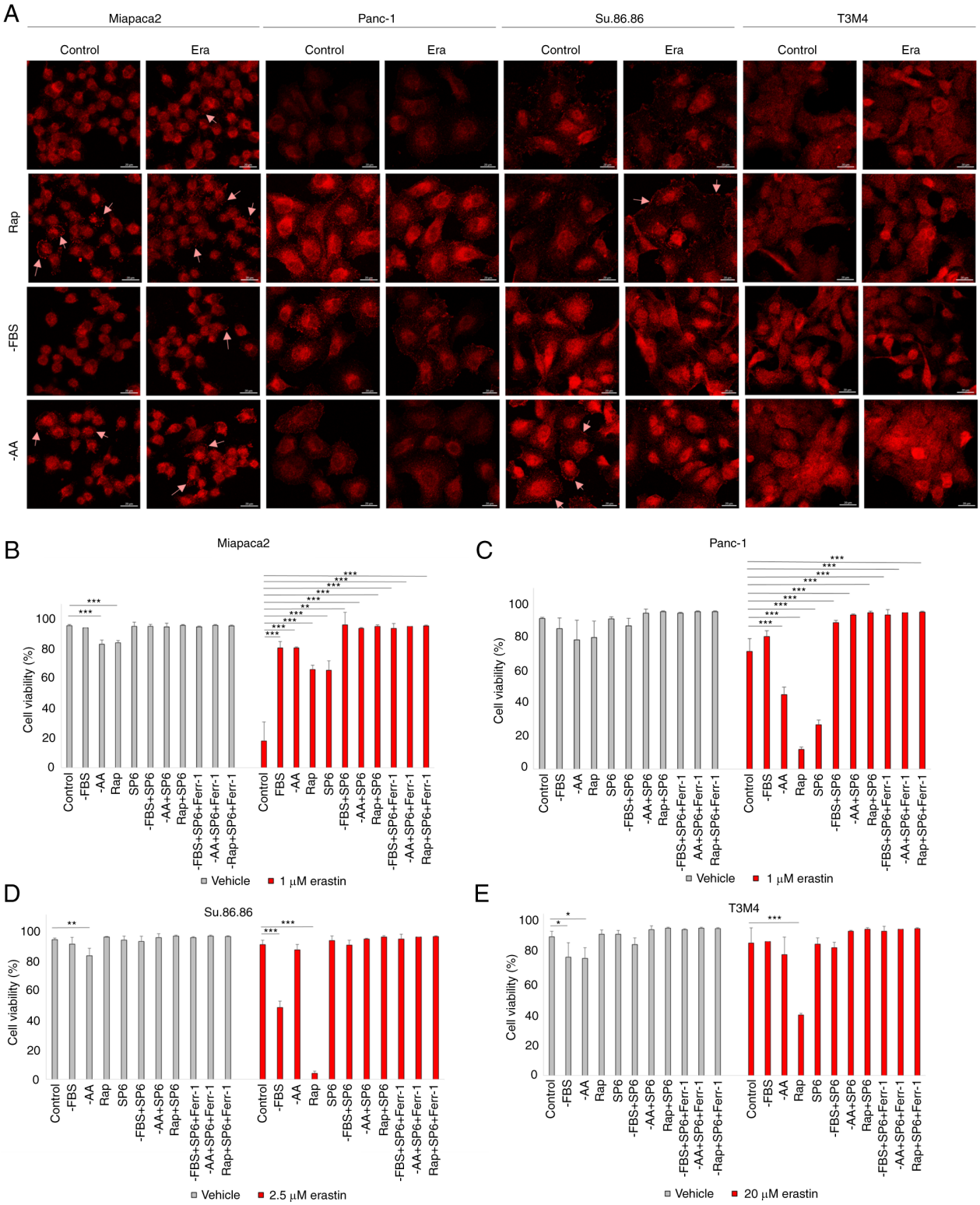

Figure 4. Starvation regulates ferroptosis via JNK. (A) Confocal microscopy images of phospho-JNK staining in (pseudo)starved Miapaca2, Panc-1, Su.86.86 and T3M4 cells, with or without erastin treatment. Arrowheads indicate phospho-JNK accumulation in the cell membrane. Scale bar, 20 μm. (B-E) Cell viability assessment of (B) Miapaca2, (C) Panc-1, (D) Su.86.86 and (E) T3M4 cells, cultured without FBS, without amino acids L-glutamine, L-lysine and L-arginine, pseudo-starved by treating with rapamycin and treated with the JNK inhibitor, SP6 (5 μM). Ferroptosis was induced by erastin and inhibited by Ferr-1. The data are presented as the mean ± SD; n=3. Cells cultured under standard conditions were used as the control. *P<0.05, **P<0.01 and ***P<0.001, vs. control. -AA, cells, cultured without L-glutamine, L-lysine and L-arginine; Rap, rapamycin; SP6, SP600125; Ferr-1, ferrostatin-1.

Discussion

Oxidative stress lies in the nature of pancreatic cancer, as known triggers of pancreatic carcinogenesis, such as alcohol consumption and inflammation, generate ROS and promote malignant lesions in the pancreas (35,36). Generally, there are two main strategies to kill cells which thrive on accumulating ROS: To deplete ROS or to elevate oxidative stress above the

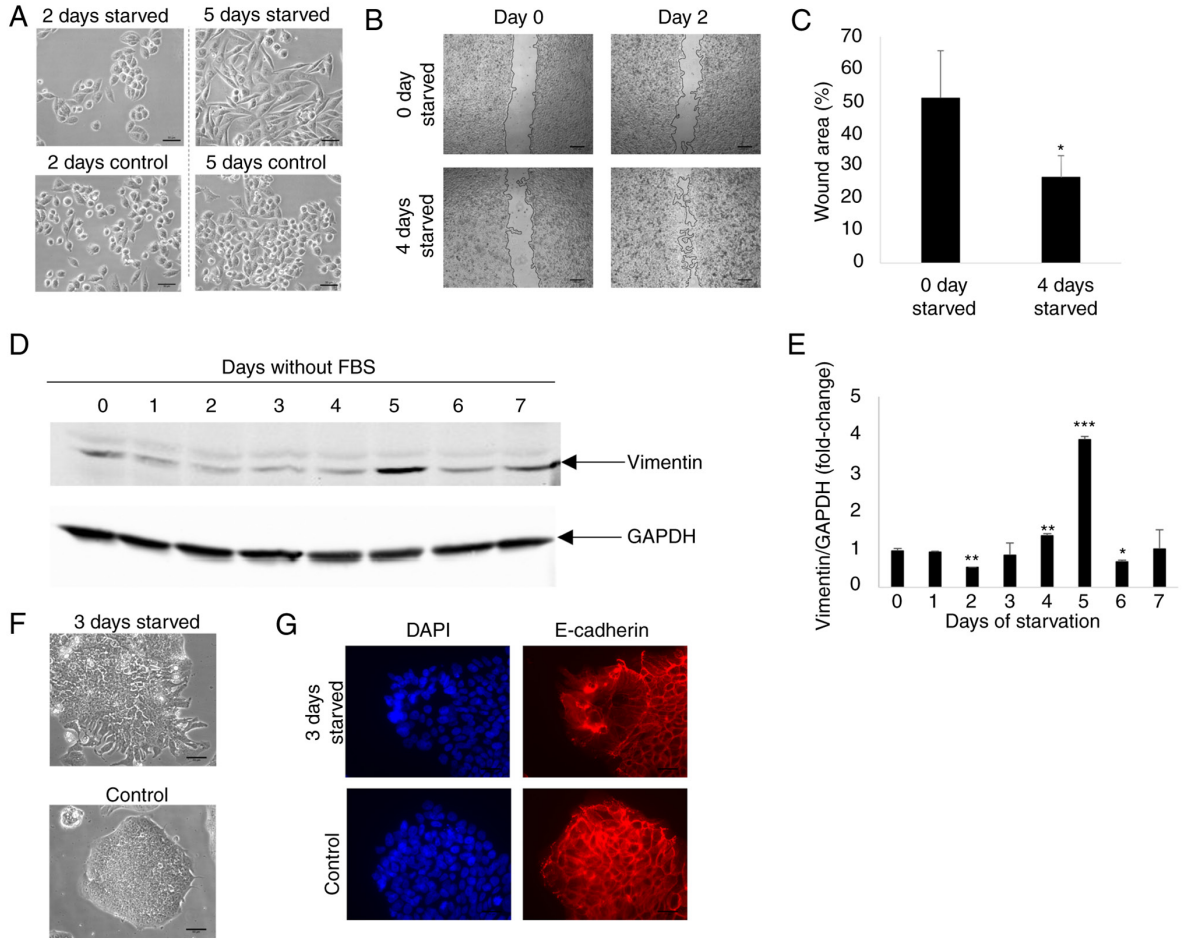

Figure 5. Pancreatic cancer cells transition between different mesenchymal states during FBS starvation. (A) Representative images of Miapaca2 cells, starved for 2 and 5 days without FBS. Scale bar, 50 μm. (B) Wound healing assay of non-starved and 4 days starved Miapaca-2 cells. Scale bar, 200 μm. (C) Quantification of the results of wound healing assay in panel B. (D) Western blot analysis of vimentin in Miapaca2 cells, starved for 1-7 days. (E) Quantification of western blots in panel D. (F) Representative images of Capan-26 cells, starved for 3 days without FBS. Scale bar, 50 μm. (G) E-cadherin immunofluorescence of starved and non-starved Capan-26 cells. Scale bar, 50 μm. The data are presented as the mean ± SD; n=3. Cells cultured under standard conditions were used as the control. *P<0.05, **P<0.01 and ***P<0.001, vs. 0 days of starvation.

bearable threshold, i.e., anti-oxidant or pro-oxidant cancer therapies. Although both have been tested for pancreatic cancer, the present study focused on the latter. In the present study, new strategies with which to improve pancreatic cancer treatment were identified by modulating ferroptosis, a unique cell death type based on membrane lipid oxidation due to iron overload. Ferroptosis is morphologically and biochemically distinct from apoptosis, necroptosis or autophagy, and has gained considerable attention since it was first identified. One of the most notable recent findings is that ferroptosis induction inhibits pancreatic cancer resistance to gemcitabine, a first-line pancreatic cancer drug (37).

Sensitivity to ferroptosis is dependent on metabolic rewiring, a common trait of pancreatic cancer, which can be exemplified by glucose and glutamine dependence. The cystine-glutamate antiporter system xc^- mediates cellular cystine import by exchanging one molecule of cystine for glutamate. In the cell, cystine is rapidly reduced to cysteine and used for glutathione biosynthesis. Cystine reduction involves nicotinamide-adenine dinucleotide phosphate (NADPH), which is generated from glucose via the pentose phosphate pathway. NADPH is also used to reduce oxidized glutathione. Cells overexpressing solute carrier family 7 member 11, a transporter component of the xc^- system, tend to be more resistant to ferroptosis inducers due to elevated levels of reduced glutathione and GPX4 activity. However, to meet energy demands and supply sufficient amounts of glutamate for the tricarboxylic acid cycle, cells need to enhance glutamate import, commonly in the form of glutamine. In this manner, ferroptosis resistance is coupled to glutamine and glucose dependency (14). Pancreatic cancer falls into a broad category of glutamine-dependent cancers, although cells use different enzymes to metabolize glutamine due to *KRAS* mediated reprogramming (15). Thus, depleting cells from nutrients, not exclusively glucose or glutamine, may have a therapeutic benefit in pancreatic cancer, which is sensitive to ferroptosis induction. This hypothesis led to the present study.

The findings of the present study indicate that treatments that induce or mimic starvation (growth factor and amino acid withdrawal, together with exposure to rapamycin) elicit contrasting effects in different pancreatic cancer cell lines. Generally, Miapaca2 cells acquired resistance to ferroptosis, while Panc-1, Su.86.86 and T3M4 cells became more sensitive. Some previous findings shed light on oxidative stress resistance in cells, encountering starvation. For example, it has previously been reported that growth factor starvation

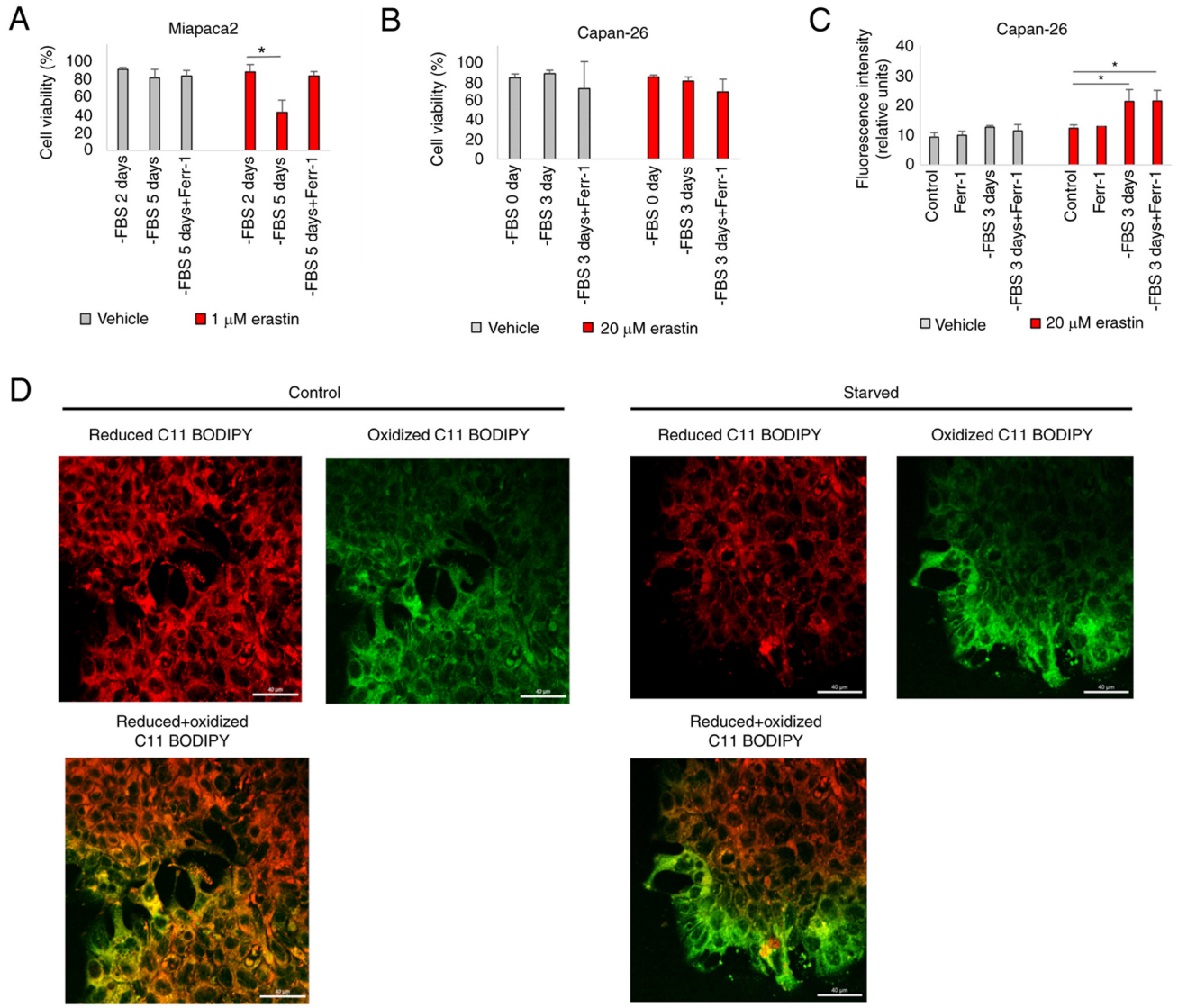

Figure 6. Transitioning between different mesenchymal states during FBS starvation alters sensitivity to ferroptosis induction. (A) Miapaca2 cell viability after reprogramming of the cells by FBS starvation for 2 and 5 days and erastin treatment. *P<0.05 vs. -FBS for 2 days. (B) Capan-26 cell viability after reprogramming of the cells by FBS starvation for 3 days and erastin treatment. (C) Measurement of lipid peroxidation of erastin treated Capan-26 cells cultured without FBS. *P<0.05 vs. control. (D) Confocal microscopy images of FBS starved and non-starved Capan-26 cells, stained with C11 BODIPY. Scale bar, 40 μm. The data are presented as the mean ± SD; n=3. Cells cultured under standard conditions were used as the control. Ferr-1, ferrostatin-1.

induces a quiescent phenotype and NF-κB activation in prostate cancer cells and protects them from ROS-induced cell death, but not specifically ferroptosis (38). Additionally, recently, Lee *et al* (39) demonstrated that energy stress inhibits ferroptosis in cancer cells through AMPK activation and the acceleration of fatty acid biosynthesis. However, in some cells encountering growth factor deprivation, AMPK activation requires gradual ROS accumulation (40). In contrast to the Panc-1 and Su.86.86 cells, the same time course of FBS and amino acid starvation increased the amount of reduced glutathione in Miapaca2 cells, indicating slower antioxidant responses (Fig. S7), which explains, at least in part, the differences in sensitivity. It has also been observed that amino acid starvation exerted an anti-ferroptotic effect on Miapaca2 cells. Sato *et al* (41) demonstrated that the deprivation of lysine, arginine and other amino acids increased cystine import and the expression of the components of cystine-glutamate antiporter xc^-, which could protect cells against ferroptosis. Even more pronounced effects to erastin sensitivity were observed in the present study following pseudo-starvation induced by treating cells with rapamycin, but not with the dual mTORC1/mTORC2 inhibitor INK128. This demonstrates the involvement of mTORC2-mediated feedback loops, as prolonged incubation with rapamycin inhibits S6K and thus, indirectly activates its downstream target Rictor and consequently mTORC2. Gu *et al* (42) indicated that active mTORC2 diminished cystine import, while the knockout or pharmacological inhibition of this protein exerted an opposite effect. This mechanism supports the current observations in Panc-1, Su.86.86 and T3M4 cells, in which rapamycin enhances erastin cytotoxicity. ERK1/2 is an established downstream target of rapamycin-induced mTORC2 feedback signaling. The results confirmed ERK1/2 translocation to the cell nucleus after rapamycin and erastin combined treatment in Miapaca2, Panc-1, Su.86.86 and T3M4 cells. Pharmacological ERK1/2 inhibition protected pancreatic cancer cells from

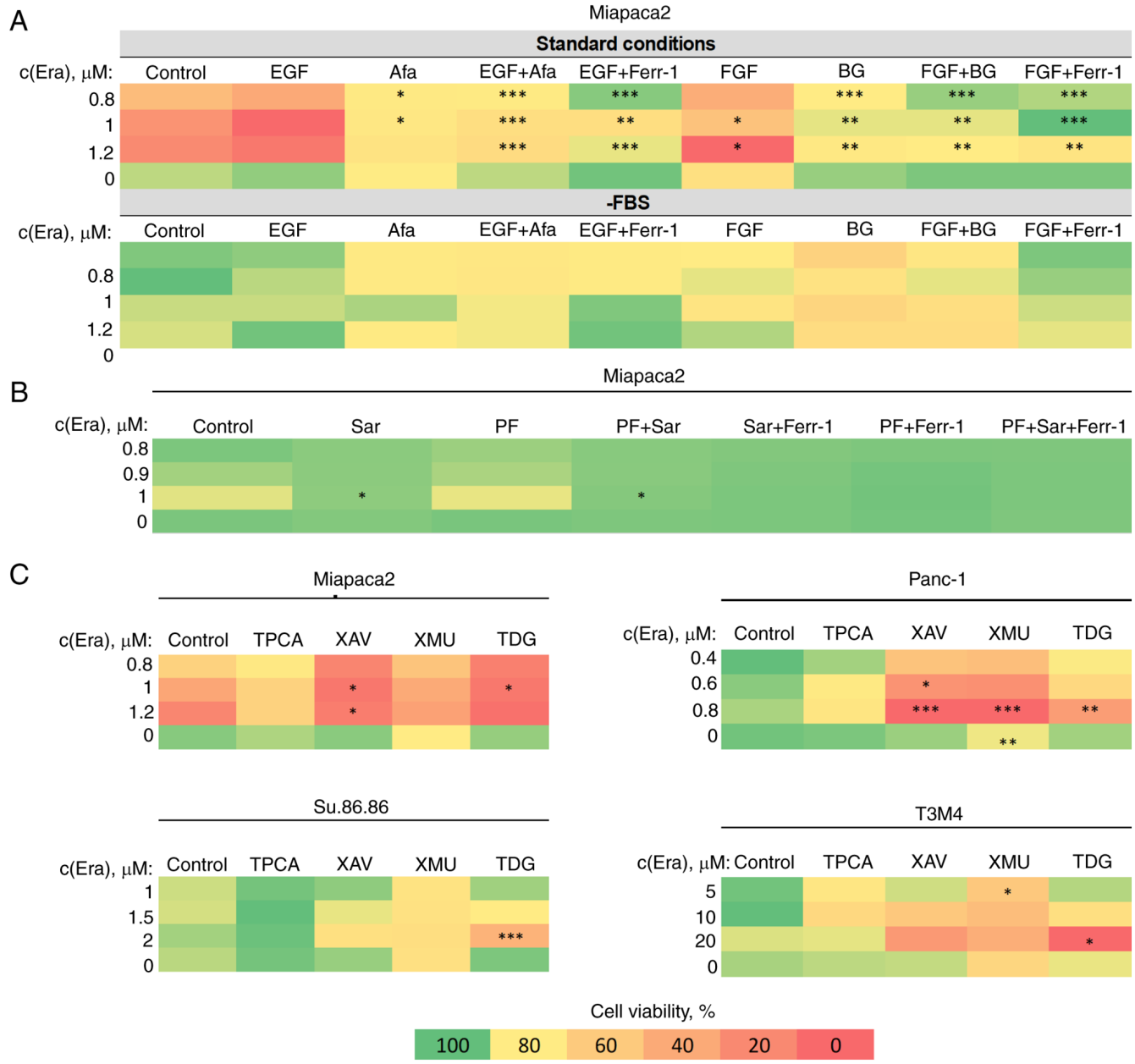

Figure 7. EMT modulation increases pancreatic cancer cell sensitivity to ferroptosis. (A) Miapaca2 cell viability following combined treatment with erastin and EMT-inducing growth factors, EGF and FGF (100 ng/ml). Afa and BG inhibited EGFR and FGFR, respectively. (B) Miapaca2 cell viability following simultaneous exposure to erastin and the EMT inhibitors, Sar and PF. (C) Combinatorial cell viability analysis of other EMT-targeting compounds and erastin in different pancreatic cancer cell lines. Cells cultured under standard conditions were used as the control. *P<0.05, **P<0.01 and ***P<0.001 vs. control (untreated) cells. EMT, epithelial-to-mesenchymal transition; Era, erastin; FGF/bFGF; basic fibroblast growth factor; Afa, afatinib; Ferr-1, ferrostatin-1; BG, BGJ398; Sar, saracatinib; PF, PF573228; TPCA, TPCA-1; XAV, XAV939; XMU, XMU-MP-1; TDG, tideglusib.

erastin-induced ferroptosis. In addition, starvation-induced resistance to erastin in pancreatic cancer cells was mediated by another kinase, JNK. Indeed, JNK was also activated in pseudo-starved and erastin-treated pancreatic cancer cells. Of note, the findings of the present study highlight a dual role of JNK in oxidative stress response regulation. In Panc-1 cells under standard conditions, JNK inhibition enhanced ROS-induced cell death; however, starvation combined with JNK inhibition protected these cells from erastin cytotoxicity. The antioxidant properties of the JNK inhibitor, SP6, were also observed in Miapaca2 cells even at nutrient-rich conditions. Although these results appear paradoxical, some insights on a pro-oxidant JNK role have been proposed; however, mainly in the context of the regulation of mitochondria function in normal cell apoptosis (43-45). With respect to ferroptosis, it has been shown that the activation of JNK and p38 elevates the expression of NADPH oxidase 4 and enhances the ferroptosis of pancreatic islet cells (46). Moreover, Yang *et al* (47) recently reported that JNK downregulated GPX4 and promoted the ferroptosis of colorectal cancer cells (46). However, none of these mechanisms is directly linked to cell metabolism. To our knowledge, the present study is the first to report the starvation-induced anti-ferroptotic role of JNK.

Nutrient withdrawal mimics conditions that cancer cells face in larger tumors before neovascularization. Poor perfusion is a common trait of pancreatic cancer tumors and it

impairs nutrient access to the deeper tumor layers (48). It is known that serum starvation enhances metastatic properties of cancer cells (49). The results of the present study demonstrated that FBS starvation induced changes in cell morphology and epithelial and mesenchymal marker expression and/or increased motility of two pancreatic cancer cell lines, Miapaca2 and Capan-26. These changes were not observed in the pancreatic cancer cell lines, Panc-1, Su.86 86 and T3M4. While starved, the Miapaca2 cells transitioned between mesenchymal-like (original) to epithelial-like to mesenchymal states. The epithelial-like state proved to be the most resistant to erastin. One possible explanation may be that, in this case, mesenchymal properties and possibly cell sensitivity are mediated by an autocrine stimulation of unknown growth factors, which elicit their effect only when their concentration is below the threshold; i.e., the concept of dependence receptors (50). From an evolutionary perspective, it may be hypothesized that gaining more epithelial properties and enhancing cell-cell junctions could help stromal cells to form a shield and protect epithelial cancer (stem) cells from oxidative damage in pancreatic tumors.

Increased mesenchymal properties under FBS starvation conditions sensitized the Miapaca2 cells to erastin-induced ferroptosis and was associated with an increased proportion of oxidized membrane lipids in Capan-26 cells. With this in mind, several EMT-targeting compounds were evaluated for their effects on cell sensitivity to erastin. As was expected, the EMT-promoting growth factors, EGF and FGF, enhanced Miapaca2 cell sensitivity to erastin, whereas blocking their receptors diminished this effect. Furthermore, the classical anti-EMT drug Src inhibitor, Sar, but not functionally related FAK inhibitor, PF, prevented erastin-induced cell death. Lastly, the inhibitors of the Wnt and Hippo signaling pathways (XAV and XMU, respectively) enhanced erastin cytotoxicity. In some cases, a biphasic inhibitory effect was observed: In Panc-1, Su.86.86 and T3M4 cells, the tankyrase inhibitor, XAV, prevented cell death at a low erastin concentration, but enhanced its cytotoxic effect at higher erastin concentrations. The GSK-3 inhibitor, tideglusib, combined with erastin, exerted the most prominent cytotoxic effect in all cell lines tested, even in T3M4 cells, which are overall resistant to erastin. From a mechanistic perspective, by inhibiting GSK-3, tideglusib indirectly activates β-catenin, which can promote EMT by blocking cell-cell junctions (51).

In recent years, cancer starvation therapies have gained considerable levels of attention. Common strategies with which to starve tumors include treatment with antiangiogenic compounds, vascular blood supply disruption, direct decomposition of intratumoral nutrients and treatment with agents that induce pseudo-starvation, such as inhibitors of growth factor receptors and the mTOR pathway (52-55). The combination of starvation and pro-oxidant therapies has proven to be effective both *in vitro* and *in vivo* (56). The present study demonstrated that in pancreatic cancer cells, starvation mediated sensitivity to ferroptosis via the ERK1/2 and JNK kinases and by inducing the transition between epithelial and mesenchymal states. Therefore, there may be some new avenues for further research, both in the basic and the clinical sciences, regarding therapies that combine kinase inhibitors, ferroptosis-inducing agents and common anti-proliferative drugs.

Acknowledgements

The authors acknowledge financial support for publishing the manuscript from Dr Violeta Jonusiene (Institute of Biosciences, Vilnius University Life Sciences Centre, Vilnius, Lithuania). The authors would also thank Dr Mindaugas Valius (Proteomics Centre, Institute of Biochemistry, Vilnius University Life Sciences Centre, Vilnius, Lithuania) for the laboratory equipment and materials.

Funding

No funding was received.

Availability of data and materials

All data generated or analyzed during this study is included in this published article or are available from the corresponding author on reasonable request.

Authors' contributions

EZ conceptualized the study. EZ and JC designed the experiments. EZ carried out the experiments. EZ and JC wrote the manuscript and confirm the authenticity of all the raw data. Both authors have read and approved the final manuscript.

Ethics approval and consent to participate

Not applicable.

Patient consent for publication

Not applicable.

Competing interests

The authors declare that they have no competing interests.

References

1. Sung H, Ferlay J, Siegel RL, Laversanne M, Soerjomataram I, Jemal A and Bray F: Global cancer statistics 2020: GLOBOCAN estimates of incidence and mortality worldwide for 36 cancers in 185 countries. CA Cancer J Clin 71: 209-249, 2021.
2. Spadi R, Brusa F, Ponzetti A, Chiappino I, Birocco N, Ciuffreda L and Satolli MA: Current therapeutic strategies for advanced pancreatic cancer: A review for clinicians. World J Clin Oncol 7: 27-43, 2016.
3. Petrillo A, Pappalardo A, Calabrese F, Tirino G, Pompella L, Ventriglia J, Laterza MM, Caterino M, Sforza V, Iranzo V, *et al*: First line nab-paclitaxel plus gemcitabine in elderly metastatic pancreatic patients: A good choice beyond age. J Gastroint Oncol 10: 910-917, 2019.
4. Sarabi M, Mais L, Oussaid N, Desseigne F, Guibert P and De La Fouchardiere C: Use of gemcitabine as a second-line treatment following chemotherapy with folfirinox for metastatic pancreatic adenocarcinoma. Oncol Lett 13: 4917-4924, 2017.
5. Ferlay J, Partensky C and Bray F: More deaths from pancreatic cancer than breast cancer in the EU by 2017. Acta Oncol 55: 1158-1160, 2016.
6. Dixon SJ, Lemberg KM, Lamprecht MR, Skouta R, Zaitsev EM, Gleason CE, Patel DN, Bauer AJ, Cantley AM, Yang WS, *et al*: Ferroptosis: An iron-dependent form of nonapoptotic cell death. Cell 149: 1060-1072, 2012.
7. Han C, Liu Y, Dai R, Ismail N, Su W and Li B: Ferroptosis and its potential role in human diseases. Front Pharmacol 11: 239, 2020.

8. Basuli D, Tesfay L, Deng Z, Paul B, Yamamoto Y, Ning G, Xian W, Mckeon F, Lynch M, Crum CP, *et al*: Iron addiction: A novel therapeutic target in ovarian cancer. Oncogene 36: 4089-4099, 2017.
9. Eling N, Reuter L, Hazin J, Hamacher-Brady A and Brady NR: Identification of artesunate as a specific activator of ferroptosis in pancreatic cancer cells. Oncoscience 2: 517-532, 2015.
10. Li B, Yang L, Peng X, Fan Q, Wei S, Yang S, Li X, Jin H, Wu B, Huang M, *et al*: Emerging mechanisms and applications of ferroptosis in the treatment of resistant cancers. Biomed Pharmacother 130: 110710, 2020.
11. Gagliardi M, Saverio V, Monzani R, Ferrari E, Piacentini M and Corazzari M: Ferroptosis: A new unexpected chance to treat metastatic melanoma? Cell Cycle 19: 2411-2425, 2020.
12. Liu H, Schreiber SL and Stockwell BR: Targeting dependency on the GPX4 lipid peroxide repair pathway for cancer therapy. Biochemistry 57: 2059-2060, 2018.
13. Viswanathan VS, Ryan MJ, Dhruv HD, Gill S, Eichhoff OM, Seashore-Ludlow B, Kaffenberger SD, Eaton JK, Shimada K, Aguirre AJ, *et al*: Dependency of a therapy-resistant state of cancer cells on a lipid peroxidase pathway. Nature 547: 453-457, 2017.
14. Koppula P, Zhuang L and Gan B: Cystine transporter SLC7A11/xCT in cancer: Ferroptosis, nutrient dependency, and cancer therapy. Protein Cell 12: 599-620, 2021.
15. Son J, Lyssiotis CA, Ying H, Wang X, Hua S, Ligorio M, Perera RM, Ferrone CR, Mullarky E, Shyh-Chang N, *et al*: Glutamine supports pancreatic cancer growth through a KRAS-regulated metabolic pathway. Nature 496: 101-105, 2013.
16. Liu Q, Zhang H, Jiang X, Qian C, Liu Z and Luo D: Factors involved in cancer metastasis: A better understanding to 'seed and soil' hypothesis. Mol Cancer 16: 176, 2017.
17. Ni B, Ghosh B, Paldy FS, Colin R, Heimerl T and Sourjik V: Evolutionary remodeling of bacterial motility checkpoint control. Cell Rep 18: 866-877, 2017.
18. Gancedo JM: Control of pseudohyphae formation in Saccharomyces cerevisiae. FEMS Microbiol Rev 25: 107-123, 2001.
19. Keenan MM and Chi JT: Alternative fuels for cancer cells. Cancer J 21: 49-55, 2015.
20. Commisso C, Davidson SM, Soydaner-Azeloglu RG, Parker SJ, Kamphorst JJ, Hackett S, Grabocka E, Nofal M, Drebin JA, Thompson CB, *et al*: Macropinocytosis of protein is an amino acid supply route in Ras-transformed cells. Nature 497: 633-637, 2013.
21. Martinez-Outschoorn UE, Lisanti MP and Sotgia F: Catabolic cancer-associated fibroblasts transfer energy and biomass to anabolic cancer cells, fueling tumor growth. Semin Cancer Biol 25: 47-60, 2014.
22. Yang S, Wang X, Contino G, Liesa M, Sahin E, Ying H, Bause A, Li Y, Stommel JM, Dell'antonio G, *et al*: Pancreatic cancers require autophagy for tumor growth. Genes Devel 25: 717-729, 2011.
23. Lugano R, Ramachandran M and Dimberg A: Tumor angiogenesis: Causes, consequences, challenges and opportunities. Cell Mol Life Sci 77: 1745-1770, 2020.
24. Prabhakar NR and Semenza GL: Adaptive and maladaptive cardiorespiratory responses to continuous and intermittent hypoxia mediated by hypoxia-inducible factors 1 and 2. Physiol Rev 92: 967-1003, 2012.
25. Kuczynski EA, Vermeulen PB, Pezzella F, Kerbel RS and Reynolds AR: Vessel co-option in cancer. Nat Rev Clin Oncol 16: 469-493, 2019.
26. Neophytou CM, Panagi M, Stylianopoulos T and Papageorgis P: The role of tumor microenvironment in cancer metastasis: Molecular mechanisms and therapeutic opportunities. Cancers (Basel) 13: 2053, 2021.
27. Janssen LME, Ramsay EE, Logsdon CD and Overwijk WW: The immune system in cancer metastasis: Friend or foe? J Immunotherapy Cancer 5: 79, 2017.
28. Wang RA, Lu YY and Fan DM: Reasons for cancer metastasis: A holistic perspective. Mol Clin Oncol 3: 1199-1202, 2015.
29. Trauzold A, Siegmund D, Schniewind B, Sipos B, Egberts J, Zorenkov D, Emme D, Röder C, Kalthoff H and Wajant H: TRAIL promotes metastasis of human pancreatic ductal adenocarcinoma. Oncogene 25: 7434-7439, 2006.
30. Jiao D, Cai Z, Choksi S, Ma D, Choe M, Kwon HN, Baik JY, Rowan BG, Liu C and Liu ZG: Necroptosis of tumor cells leads to tumor necrosis and promotes tumor metastasis. Cell Res 28: 868-870, 2018.
31. Zalyte E, Dedonyte V, Kurlinkus B, Sileikis A, Schemmer P and Valius M: Establishment and characterization of a new pancreatic ductal adenocarcinoma cell line capan-26. Anticancer Res 41: 1401-1406, 2021.
32. Ger M, Žalytė E, Kaupinis A, Kurlinkus B, Petrulionis M, Šileikis A, Strupas K and Valius M: Primary pancreatic ductal adenocarcinoma cell cultures represent the features of native tumours. Biologija 65: 20-33, 2019.
33. Rabanal-Ruiz Y, Otten EG and Korolchuk VI: mTORC1 as the main gateway to autophagy. Essays Biochem 61: 565-584, 2017.
34. Soares HP, Ni Y, Kisfalvi K, Sinnett-Smith J and Rozengurt E: Different patterns of Akt and ERK feedback activation in response to rapamycin, active-site mTOR inhibitors and metformin in pancreatic cancer cells. PLoS One 8: e57289, 2013.
35. Liou GY, Döppler H, DelGiorno KE, Zhang L, Leitges M, Crawford HC, Murphy MP and Storz P: Mutant kras-induced mitochondrial oxidative stress in acinar cells upregulates EGFR signaling to drive formation of pancreatic precancerous lesions. Cell Rep 14: 2325-2336, 2016.
36. Palmieri VO, Grattagliano I and Palasciano G: Ethanol induces secretion of oxidized proteins by pancreatic acinar cells. Cell Biol Toxicol 23: 459-464, 2007.
37. Zhu S, Zhang Q, Sun X, Zeh HJ III, Lotze MT, Kang R and Tang D: HSPA5 regulates ferroptotic cell death in cancer cells. Cancer Res 77: 2064-2077, 2017.
38. White EZ, Pennant NM, Carter JR, Hawsawi O, Odero-Marah V and Hinton CV: Serum deprivation initiates adaptation and survival to oxidative stress in prostate cancer cells. Sci Rep 10: 12505, 2020.
39. Lee H, Zandkarimi F, Zhang Y, Meena JK, Kim J, Zhuang L, Tyagi S, Ma L, Westbrook TF, Steinberg GR, *et al*: Energy-stress-mediated AMPK activation inhibits ferroptosis. Nat Cell Biol 22: 225-234, 2020.
40. Wu CA, Chao Y, Shiah SG and Lin WW: Nutrient deprivation induces the warburg effect through ROS/AMPK-dependent activation of pyruvate dehydrogenase kinase. Biochimica et biophysica Acta 1833: 1147-1156, 2013.
41. Sato H, Nomura S, Maebara K, Sato K, Tamba M and Bannai S: Transcriptional control of cystine/glutamate transporter gene by amino acid deprivation. Biochem Biophysical Res Communicati 325: 109-116, 2004.
42. Gu Y, Albuquerque CP, Braas D, Zhang W, Villa GR, Bi J, Ikegami S, Masui K, Gini B, Yang H, *et al*: mTORC2 regulates amino acid metabolism in cancer by phosphorylation of the cystine-glutamate antiporter xCT. Mol Cell 67: 128-138 e127, 2017.
43. Hanawa N, Shinohara M, Saberi B, Gaarde WA, Han D and Kaplowitz N: Role of JNK translocation to mitochondria leading to inhibition of mitochondria bioenergetics in acetaminophen-induced liver injury. J Biol Chem 283: 13565-13577, 2008.
44. Win S, Than TA, Le BH, Garcia-Ruiz C, Fernandez-Checa JC and Kaplowitz N: Sab (Sh3bp5) dependence of JNK mediated inhibition of mitochondrial respiration in palmitic acid induced hepatocyte lipotoxicity. J Hepatol 62: 1367-1374, 2015.
45. Lee YH, Govinda B, Kim JC, Kim TI, Lee NH, Lee JC, Yi HK and Jhee EC: Oxidative stress resistance through blocking Hsp60 translocation followed by SAPK/JNK inhibition in aged human diploid fibroblasts. Cell Biochem Funct 27: 35-39, 2009.
46. Li XY and Leung PS: Erastin-induced ferroptosis is a regulator for the growth and function of human pancreatic islet-like cell clusters. Cell Regen 9: 16, 2020.
47. Yang Y, Lin Z, Han Z, Wu Z, Hua J, Zhong R, Zhao R, Ran H, Qu K, Huang H, *et al*: miR-539 activates the SAPK/JNK signaling pathway to promote ferropotosis in colorectal cancer by directly targeting TIPE. Cell Death Dis 7: 272, 2021.
48. Kamphorst JJ, Nofal M, Commisso C, Hackett SR, Lu W, Grabocka E, Vander Heiden MG, Miller G, Drebin JA, Bar-Sagi D, *et al*: Human pancreatic cancer tumors are nutrient poor and tumor cells actively scavenge extracellular protein. Cancer Res 75: 544-553, 2015.
49. Tong H, Yin H, Hossain MA, Wang Y, Wu F, Dong X, Gao S, Zhan K and He W: Starvation-induced autophagy promotes the invasion and migration of human bladder cancer cells via TGF-β1/Smad3-mediated epithelial-mesenchymal transition activation. J Cell Biochem 120: 5118-5127, 2019.
50. Stone TW: Dependence and guidance receptors-DCC and Neogenin-in partial EMT and the actions of serine proteases. Front Oncol 10: 94, 2020.

51. Kim WK, Kwon Y, Jang M, Park M, Kim J, Cho S, Jang DG, Lee WB, Jung SH, Choi HJ, *et al*: β-catenin activation down-regulates cell-cell junction-related genes and induces epithelial-to-mesenchymal transition in colorectal cancers. Sci Rep 9: 18440, 2019.
52. Coppock JD, Vermeer PD, Vermeer DW, Lee KM, Miskimins WK, Spanos WC and Lee JH: mTOR inhibition as an adjuvant therapy in a metastatic model of HPV+ HNSCC. Oncotarget 7: 24228-24241, 2016.
53. Chan DLH, Segelov E, Wong RS, Smith A, Herbertson RA, Li BT, Tebbutt N, Price T and Pavlakis N: Epidermal growth factor receptor (EGFR) inhibitors for metastatic colorectal cancer. Cochrane Database Syst Rev 6: CD007047, 2017.
54. Demkova L and Kucerova L: Role of the HGF/c-MET tyrosine kinase inhibitors in metastasic melanoma. Mol Cancer 17: 26, 2018.
55. Yu S, Chen Z, Zeng X, Chen X and Gu Z: Advances in nanomedicine for cancer starvation therapy. Theranostics 9: 8026-8047, 2019.
56. D'Aronzo M, Vinciguerra M, Mazza T, Panebianco C, Saracino C, Pereira SP, Graziano P and Pazienza V: Fasting cycles potentiate the efficacy of gemcitabine treatment in in vitro and in vivo pancreatic cancer models. Oncotarget 6: 18545-18557, 2015.